SUPPLEMENTARY INFORMATION

Unraveling the electric field-induced second harmonic generation responses of stilbazolium ion pairs complexes in solution using a multiscale simulation method

*Tárcius N. Ramos[1,2], Sylvio Canuto[1], Benoît Champagne[2]**

[1] Universidade de Sao Paulo, Instituto de Fisica, Rua do Matão 1371, 05508-090, São Paulo, SP, Brazil.

[2] Theoretical Chemistry Lab, Unit of Theoretical and Structural Physical Chemistry, Namur Institute of Structured Matter, University of Namur, rue de Bruxelles, 61, B-5000 Namur, Belgium.

* Email: benoit.champagne@unamur.be

Table S1. Basis set effects on the $\left[\mu\beta_{//}\right]_{eff}$ (10^{-48} esu) response at 1907 nm as determined at the IEFPCM/TD-DFT/M06-2X for complexes **1-4** and different counterion positions.

Basis set	**1**		**2**		**3**		**4**	
	In plane	Out of plane	In plane	Out of plane	In plane	Out of plane	In plane	Out of plane
6-311+G(d)	227.3	58.6	520.3	151.8	2206.3	1061.1	2285.1	1301.5
6-311+G(d,p)	225.4	58.0	522.0	153.6	2227.1	1074.6	2308.1	1317.4
aug-cc-pVDZ	219.1	60.4	516.7	155.6	2256.3	1096.4	2345.8	1352.3

Table S2. Root-mean-square deviations (RMSD) between the atomic positions of the minimum energy geometries evaluated at the ωB97X-D level and those obtained at the MP2 and re-parameterized OPLS-AA (in parenthesis) levels. BLA and the d_{NA} values obtained from MP2, ωB97X-D and OPLS-AA optimized geometries. All values are given in Å. The molecules were aligned using the quaternion algorithm.

Complex	Atomic positions	BLA			d_{NA}		
	RMSD	MP2	ωB97X-D	OPLS-AA	MP2	ωB97X-D	OPLS-AA
1	0.04 (0.14)	0.111	0.117	0.117	4.35	4.50	4.49
2	0.05 (0.13)	0.099	0.115	0.115	4.35	4.50	4.58
3	0.19 (0.16)	0.090	0.098	0.096	4.35	4.51	4.58
4	(0.23)	-	0.095	0.096	-	4.51	4.49
4.1	(0.19)	-	0.095	0.096	-	3.37	3.45
4.2	(0.20)	-	0.098	0.101	-	3.49	3.50
4.3	(0.22)	-	0.098	0.099	-	3.49	3.58
4.4	(0.21)	-	0.101	0.102	-	3.53	3.46

Table S3. IEFPCM/TD-DFT/M06-2X/6-311+G(d) EFISHG and HRS first hyperpolarizabilities at 1907 nm as a function of method to optimize the geometry and of the position of the anion. The reported quantities are $\mu\beta_{//}$ (10^3 a.u.), $\beta_{//}$ (a.u.), μ (a.u.), the $\theta_{(\mu,\beta)}$ is angle between the μ and β vectors (deg), β_{HRS} (a.u.) and its depolarization ratio (DR).

Complex	Geometry optimization	Anion position	$\mu\beta_{//}$	$\beta_{//}$	μ	$\theta_{(\mu,\beta)}$	β_{HRS}	DR
1	MP2	In plane	25.00	2954	8.46	58.8	4080	4.48
	MP2	Out of plane	4.71	769	6.13	81.1	3629	4.26
	ωB97X-D	In plane	23.48	2659	8.83	60.1	3822	4.46
	ωB97X-D	Out of plane	4.93	750	6.57	81.0	3485	4.31
2	MP2	In plane	57.54	6270	9.18	44.6	6232	4.64
	MP2	Out of plane	13.42	2151	6.24	74.1	5615	4.51
	ωB97X-D	In plane	54.72	5744	9.53	45.5	5796	4.63
	ωB97X-D	Out of plane	14.45	2141	6.75	73.4	5354	4.51
3	MP2	In plane	196.69	19071	10.31	37.1	16746	4.78
	MP2	Out of plane	82.76	11392	7.27	58.0	15108	4.72
	ωB97X-D	In plane	235.21	21326	11.03	36.5	18586	4.78
	ωB97X-D	Out of plane	110.30	14194	7.77	54.9	17320	4.76
4	ωB97X-D	In plane	242.48	22975	10.55	44.5	22477	4.82
	ωB97X-D	Out of plane	135.20	17348	7.79	54.4	20867	4.80
4.1	ωB97X-D	Out of plane	155.23	20424	7.60	45.4	20259	4.86
4.2	ωB97X-D	Out of plane	135.47	18054	7.50	51.7	20305	4.86
4.3	ωB97X-D	Out of plane	94.25	13996	6.73	60.3	19770	4.78
4.4	ωB97X-D	Out of plane	114.97	20308	5.66	41.1	18804	4.83

Table S4. Analyses of EFISHG responses at 1907 nm as determined at the IEFPCM/TD-DFT/M06-2X/6-311+G(d) level as a function of method to optimize the geometry and of the position of the anion. The following quantities are considered: $\mu\beta_{//}/kT$, $\gamma_{//}$ and γ_{EFISHG} (10^4 a.u.); $[\mu\beta_{//}]_{eff}$ (10^{-48} esu), $R_{3/2} = (3kT \times \gamma_{//})/\mu\beta_{//}$. T=298.15 K, 3kT=2.833 × 10^{-3} a.u.

Complex	Geometry optimization	Anion position	$\mu\beta_{//}/3kT$	$\gamma_{//}$	γ_{EFISHG}	$R_{3/2}$	$[\mu\beta_{//}]_{eff}$
1	MP2	In plane	883	52.1	935	0.06	242.2
	MP2	Out of plane	166	56.7	223	0.34	57.8
	ωB97X-D	In plane	829	48.3	877	0.06	227.3
	ωB97X-D	Out of plane	174	52.0	226	0.30	58.6
2	MP2	In plane	2031	82.2	2114	0.04	547.8
	MP2	Out of plane	474	82.0	556	0.17	144
	ωB97X-D	In plane	1931	75.6	2007	0.04	520.3
	ωB97X-D	Out of plane	510	75.7	586	0.15	151.8
3	MP2	In plane	6944	200.1	7144	0.03	1851.5
	MP2	Out of plane	2922	189.6	3111	0.06	806.4
	ωB97X-D	In plane	8304	208.8	8513	0.03	2206.3
	ωB97X-D	Out of plane	3894	200.5	4094	0.05	1061.1
4	ωB97X-D	In plane	8560	256.7	8817	0.03	2285.1
	ωB97X-D	Out of plane	4773	248.7	5022	0.05	1301.5
4.1	ωB97X-D	Out of plane	5480	227.5	5708	0.04	1420.3
4.2	ωB97X-D	Out of plane	4783	230.1	5013	0.05	1239.5
4.3	ωB97X-D	Out of plane	3327	228.4	3556	0.07	862.3
4.4	ωB97X-D	Out of plane	4059	221.5	4280	0.05	1051.9

Table S5. Charge analysis for complex **1** as a function of the method for geometry optimization (MP2 versus ωB97X-D) where the anion lies in the same plane as the cation ring. All results were obtained employing IEFPCM/M06-2X/aug-cc-pVDZ/CHELPG and are given in *e*.

	Atom	MP2	ωB97X-D	Δ(MP2 - ωB97X-D)
1	C	0.14	0.11	0.03
2	C	-0.33	-0.28	-0.06
3	C	0.42	0.36	0.06
4	C	-0.32	-0.29	-0.03
5	C	0.10	0.08	0.02
6	H	0.12	0.13	0.00
7	H	0.20	0.18	0.02
8	H	0.18	0.18	0.00
9	H	0.15	0.15	0.00
10	C	-0.31	-0.25	-0.06
11	C	-0.13	-0.17	0.03
12	C	0.20	0.25	-0.05
13	C	-0.19	-0.23	0.03
14	C	-0.21	-0.24	0.04
15	C	-0.06	-0.03	-0.03
16	H	0.13	0.13	-0.01
17	C	-0.05	-0.01	-0.04
18	H	0.13	0.14	0.00
19	C	-0.10	-0.14	0.04
20	H	0.10	0.10	0.00
21	H	0.10	0.09	0.01
22	H	0.10	0.11	-0.01
23	H	0.17	0.15	0.02
24	H	0.15	0.15	0.00
25	C	-0.11	-0.09	-0.01
26	H	0.09	0.09	0.00
27	H	0.12	0.11	0.01
28	H	0.10	0.09	0.00
29	N	0.02	0.04	-0.02
30	I	-0.90	-0.91	0.01

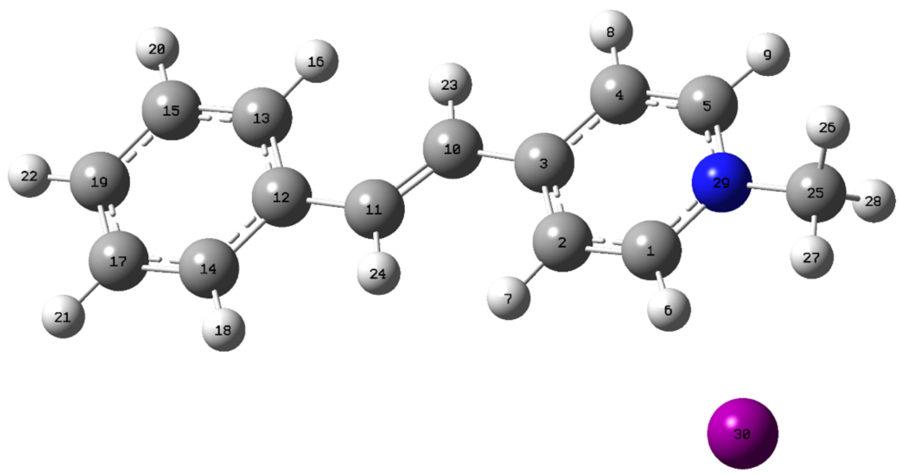

Table S6. Charge analysis for complex **2** as a function of the method for geometry optimization (MP2 versus ωB97X-D) where the anion lies in the same plane as the cation ring. All results were obtained employing IEFPCM/M06-2X/aug-cc-pVDZ/CHELPG and are given in *e*.

	Atom	MP2	ωB97X-D	Δ(MP2 - ωB97X-D)			Atom	MP2	ωB97X-D	Δ(MP2 - ωB97X-D)
1	C	0.07	0.08	-0.01		22	H	0.17	0.17	0.00
2	C	-0.28	-0.29	0.01		23	H	0.14	0.13	0.01
3	C	0.36	0.37	-0.01		24	C	-0.11	-0.09	-0.02
4	C	-0.29	-0.30	0.01		25	H	0.10	0.10	0.00
5	C	0.14	0.15	-0.01		26	H	0.10	0.09	0.00
6	H	0.15	0.14	0.01		27	H	0.12	0.10	0.01
7	H	0.18	0.18	0.00		28	N	0.02	0.02	0.00
8	H	0.18	0.18	0.00		29	I	-0.89	-0.91	0.01
9	H	0.12	0.12	0.01		30	C	0.37	0.36	0.01
10	C	-0.28	-0.29	0.01		31	C	-0.26	-0.23	-0.03
11	C	-0.14	-0.12	-0.02		32	H	0.04	0.04	0.01
12	C	0.18	0.19	-0.01		33	H	0.07	0.07	0.01
13	C	-0.16	-0.17	0.01		34	H	0.03	0.02	0.01
14	C	-0.20	-0.20	0.00		35	C	-0.22	-0.28	0.06
15	C	-0.18	-0.18	0.00		36	H	0.05	0.07	-0.02
16	H	0.12	0.12	0.00		37	H	0.04	0.06	-0.02
17	C	-0.12	-0.15	0.02		38	H	0.04	0.06	-0.02
18	H	0.13	0.13	0.00		39	C	-0.22	-0.22	0.00
19	C	0.03	0.07	-0.03		40	H	0.02	0.02	0.00
20	H	0.15	0.15	0.00		41	H	0.06	0.06	0.00
21	H	0.12	0.12	0.00		42	H	0.04	0.04	0.00

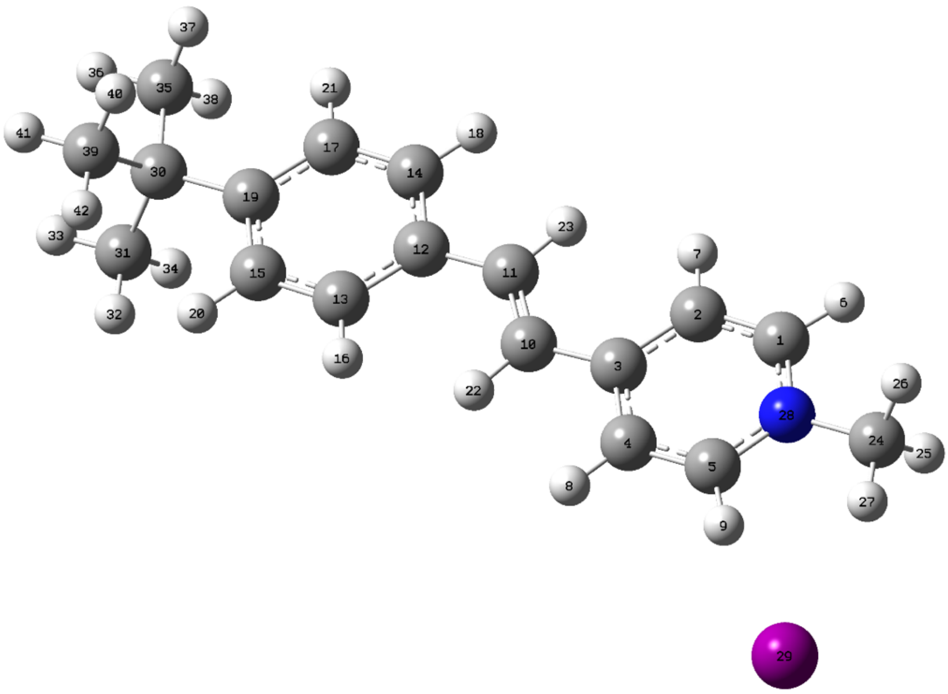

Table S7. Charge analysis for complex **3** as a function of the method for geometry optimization (MP2 versus ωB97X-D) where the anion lies in the same plane as the cation ring. All results were obtained employing IEFPCM/M06-2X/aug-cc-pVDZ/CHELPG and are given in *e*.

	Atom	MP2	ωB97X-D	Δ(MP2 - ωB97X-D)			Atom	MP2	ωB97X-D	Δ(MP2 - ωB97X-D)
1	C	0.06	0.06	0.00		20	H	0.16	0.15	0.01
2	C	-0.29	-0.30	0.01		21	H	0.16	0.15	0.01
3	C	0.38	0.39	-0.01		22	H	0.17	0.16	0.00
4	C	-0.30	-0.31	0.01		23	H	0.13	0.13	0.00
5	C	0.12	0.13	-0.01		24	C	-0.08	-0.10	0.02
6	H	0.15	0.15	0.00		25	H	0.09	0.09	0.00
7	H	0.18	0.18	0.00		26	H	0.09	0.09	-0.01
8	H	0.17	0.18	0.00		27	H	0.11	0.11	0.00
9	H	0.13	0.12	0.01		28	N	0.02	0.03	-0.02
10	C	-0.32	-0.32	0.00		29	I	-0.90	-0.91	0.01
11	C	-0.12	-0.12	0.00		30	N	-0.41	-0.25	-0.17
12	C	0.14	0.14	0.00		31	C	0.15	0.05	0.10
13	C	-0.15	-0.15	0.00		32	H	0.00	0.02	-0.02
14	C	-0.19	-0.19	0.00		33	H	0.05	0.07	-0.02
15	C	-0.28	-0.25	-0.03		34	H	0.00	0.02	-0.02
16	H	0.13	0.13	0.00		35	C	0.09	0.04	0.05
17	C	-0.25	-0.23	-0.02		36	H	0.06	0.07	-0.01
18	H	0.14	0.13	0.01		37	H	0.01	0.02	0.00
19	C	0.39	0.30	0.09		38	H	0.01	0.02	-0.01

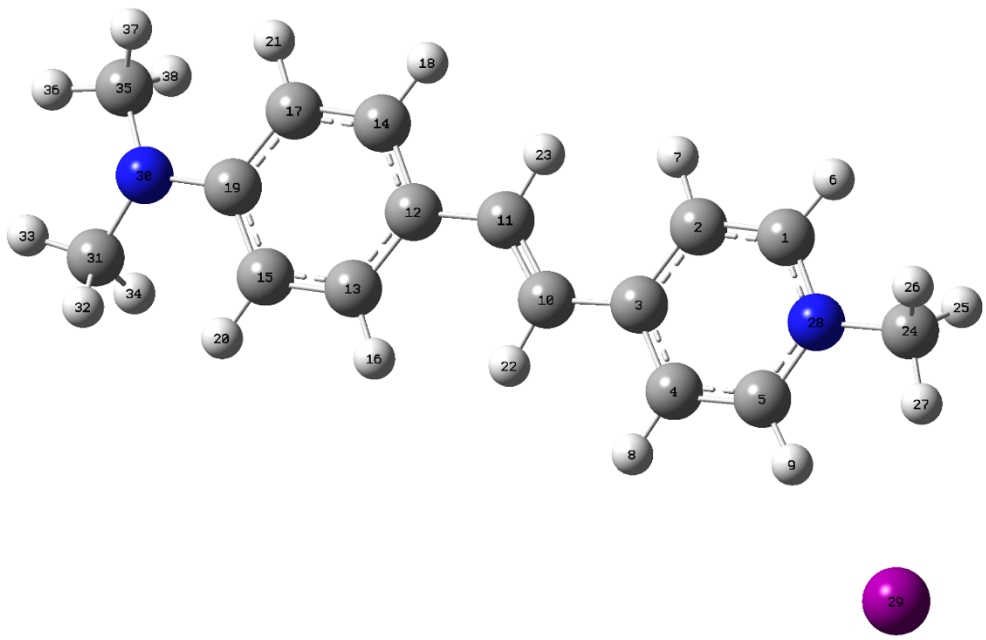

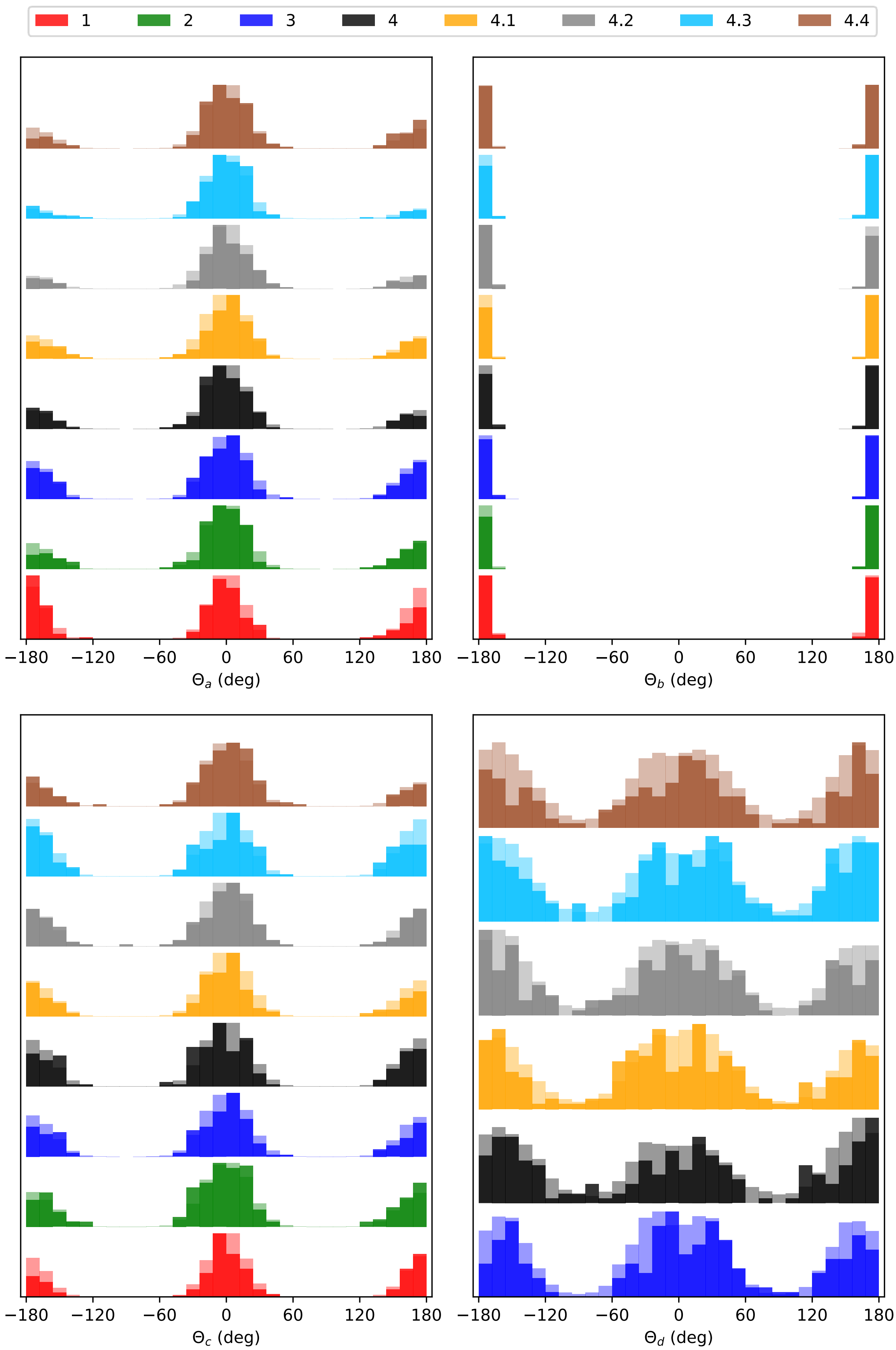

Figure S1. Distribution of the angles θ_a, θ_b, θ_c, and θ_d of the whole simulation (translucent) and of the 200 sampled configurations (opaque).

Complex **1**

HOMO-3

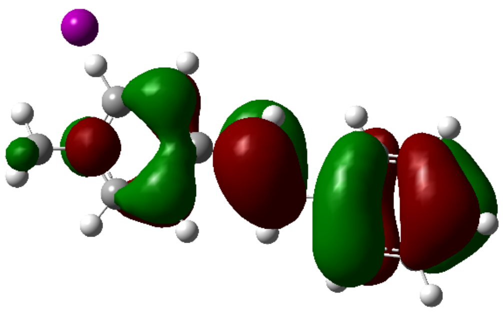

LUMO

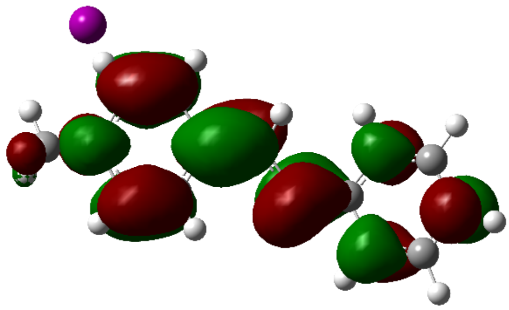

Complex **2**

HOMO-3

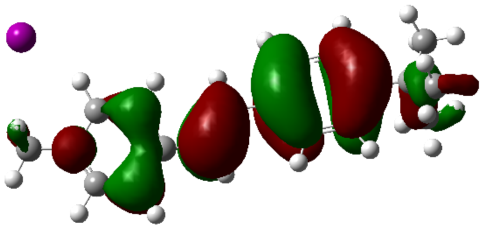

LUMO

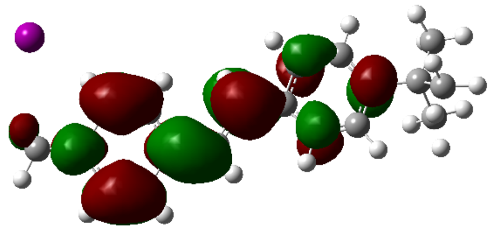

Complex **3**

HOMO

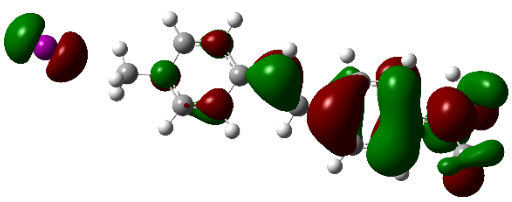

LUMO

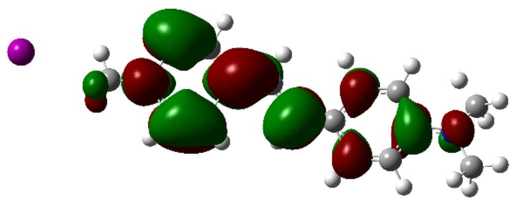

Complex **4**

HOMO

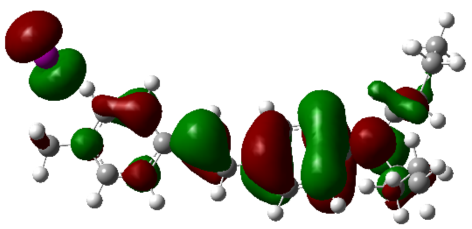

LUMO

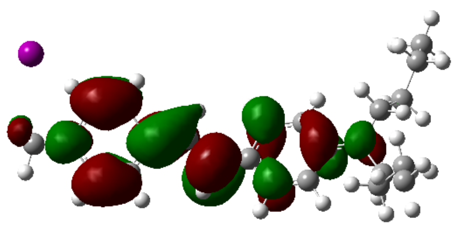

Continue.

Continue.

Complex **4.1**

HOMO LUMO

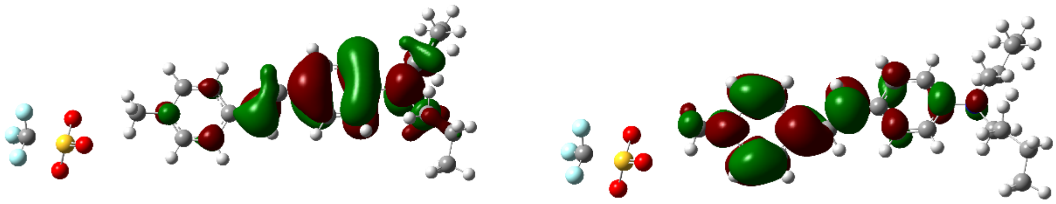

Complex **4.2**

HOMO LUMO

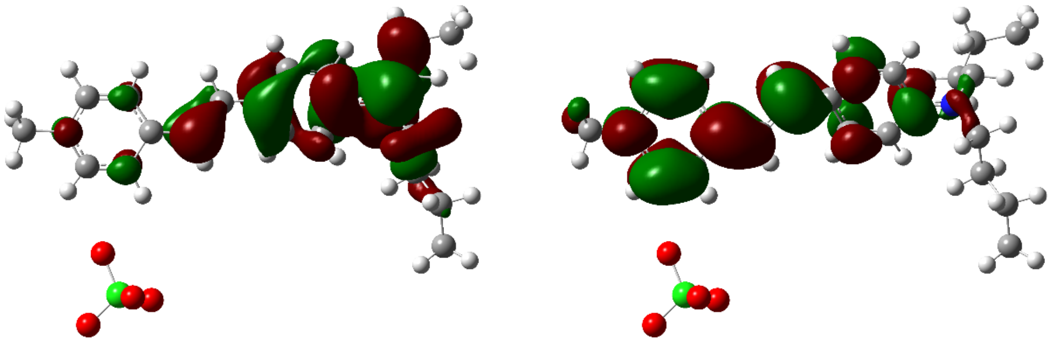

Complex **4.3**

HOMO-2 LUMO

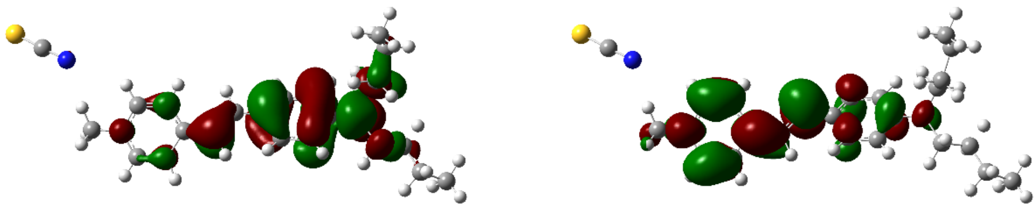

Complex **4.4**

HOMO LUMO

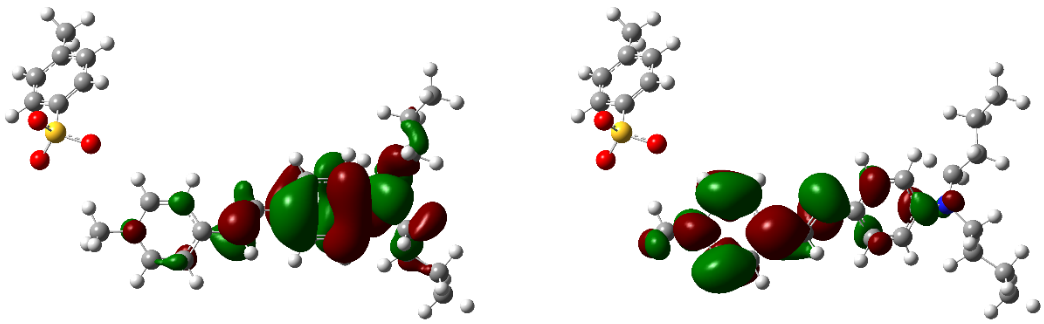

Figure S2. Main molecular orbitals involved in the dominant low-energy excitation obtained at the IEFPCM/TD-DFT/M06-2X/6-311+G(d) level. The snapshots were selected randomly from the sampled configurations.

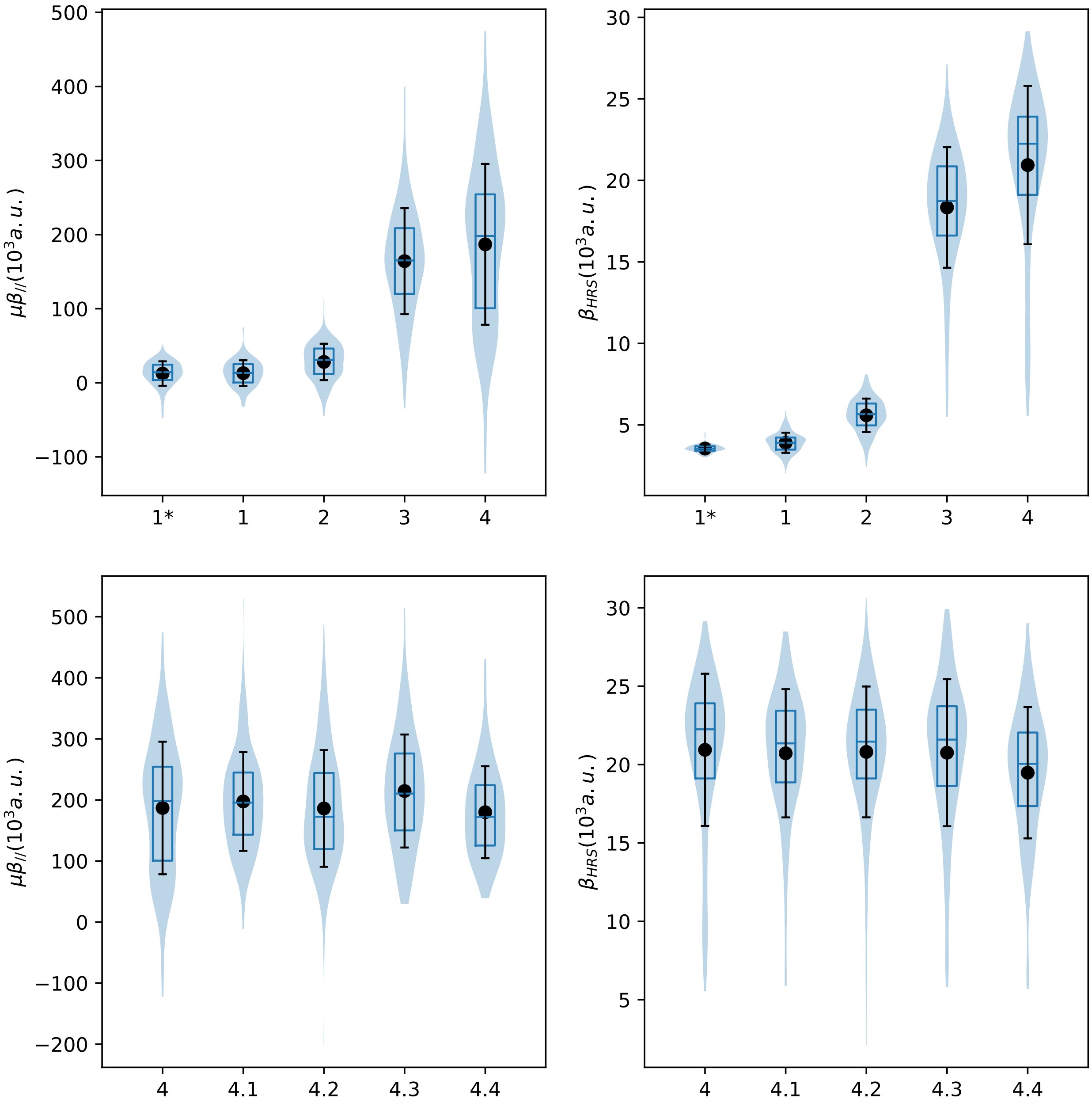

Figure S3. Violin distribution plots for $\mu\beta_{//}$ and β_{HRS}, including the average (black point), the standard deviation (black lines) and the boxplot (blue lines indicating the first quartile at 25%, the median and the third quartile at 75%). The calculations were performed at the IEFPCM/TD-DFT/M06-2X/6-311+G(d) level.

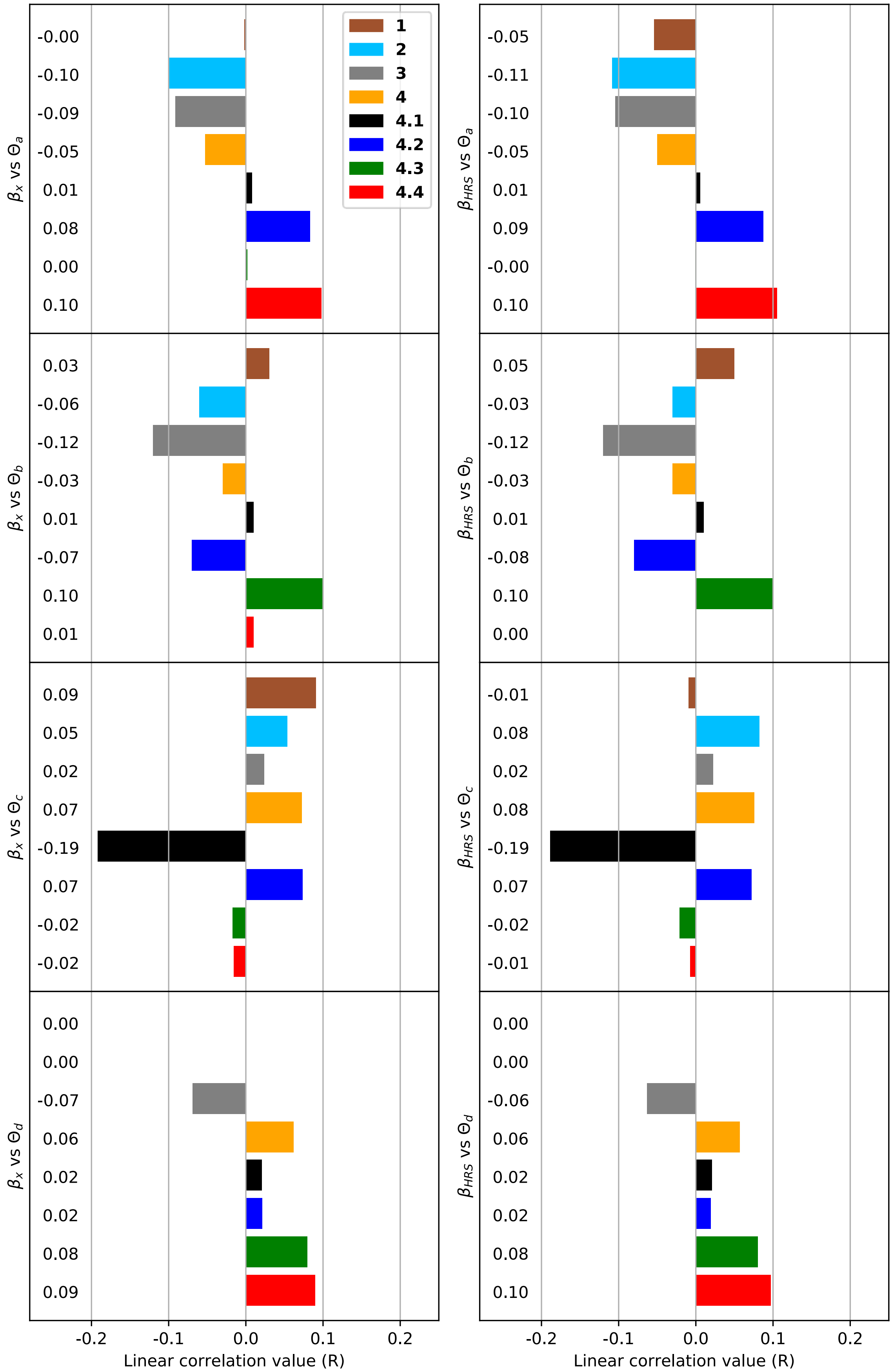

Figure S4 Linear correlation analyses for β_x and β_{HRS} *versus* the θ_a, θ_b, θ_c, and θ_d torsion angles.